All-Photonic Molecular Half-Adder

Joakim Andréasson,*,† Stephen D. Straight,‡ Gerdenis Kodis,‡ Choong-Do Park,‡ Michael Hambourger,‡ Miguel Gervaldo,‡ Bo Albinsson,*,† Thomas A. Moore,*,‡ Ana L. Moore*,‡ and Devens Gust*,‡

Department of Chemical and Biological Engineering, Physical Chemistry, Chalmers University of Technology, SE-412 96 Göteborg, Sweden, and Center for the Study of Early Events in Photosynthesis, Department of Chemistry and Biochemistry, Arizona State University, Tempe, AZ, 85287, USA

E-mail: a-son@chalmers.se or gust@asu.edu

RECEIVED DATE (to be automatically inserted after your manuscript is accepted if required according to the journal that you are submitting your paper to)

Abstract: One molecule acts as both an AND and an XOR Boolean logic gate that share the same two photonic inputs. The molecule comprises a half-adder, adding two binary digits with only light as inputs and outputs, and consists of three covalently linked photochromic moieties; a spiropyran and two quinoline-derived dihydroindolizines. The AND function is based on the absorption properties of the molecule, whereas the XOR function is based on an off-on-off response of the fluorescence to the inputs that results from interchromophore excited state quenching interactions. The half-adder is simple to operate, and can be cycled many times.

† Chalmers University of Technology

‡ Arizona State University

Introduction

Many molecules can act as switches, changing structure among two or more states as a result of stimuli. This phenomenon may be harnessed to design molecules that respond to combinations of inputs in ways that correspond to Boolean logic operations, providing a potential basis for molecule-based computing. Arithmetic operations require combinations of two or more logic gates that carry out addition or subtraction. A number of molecular half-adders[1-7] and half-subtractors[4,5,8,9] have been described, or discussed theoretically.[10,11] These function through chemical inputs (e.g., acid, base, ions) that cause the switching operations. Chemical inputs are versatile and simple to implement in demonstrations of principle, but require physical access to the molecules, operate at speeds limited by molecular diffusion, require a solution phase, and lead to an increase in solution volume and buildup of salts or other byproducts after repeated cycling of the device. Molecular switches that use solely light as inputs and outputs avoid these problems. We have reported a variety of all-photonic switches and logic gates based on photochromic molecules. Photochromes photoisomerize between two forms upon exposure to light of various wavelengths.[1,12-18] We recently reported a photonic half-adder based on two molecular logic gates and a third-harmonic-generating crystal.[1] Tian and coworkers have described a possible approach to a photochemically-driven half-adder based on a rotaxane,[6] although the function of the XOR gate portion requires reading different outputs, depending upon which inputs were applied. Here, we report a molecular triad consisting of two different photochromes: a spiropyran and a quinoline-derived dihydroindolizine. Using two inputs of ultraviolet light, the molecule functions as an AND gate via its absorption spectrum and an XOR gate through its fluorescence properties. The XOR gate operates through a non-linear, sometimes called "neuronal," response to light that involves interchromophore excited state quenching. The combination of these two gate functions produces a half-adder with simple optical inputs and readouts.

Results and Discussion

We will first describe the performance of the half-adder, in order to give the reader a general understanding of how it works, and then discuss the functional details. A Boolean half-adder, characterized by truth Table 1, carries out binary addition of two digits. It consists of an AND logic gate and an XOR gate that share two inputs, *A* and *B*. These inputs represent two binary numbers (*0* or *1*). The AND gate, which generates the carry digit, yields an *on* response only when both inputs are *on*. The XOR (exclusive OR) gate produces the sum digit, and generates an *on* response when either *A* or *B* is *on*, but not when both inputs are *on*.

Half-adder molecule **122** (Figure 1) consists of three photochromes linked to a central benzene, which

Table 1. Truth Table for the Half-Adder

Input *A*	Input *B*	Output *X*	Output *Y*	Binary sum
λ = 355 nm	λ = 355 nm	(*A* @ 581 nm) AND gate (carry digit)	(Em. @ 690 nm) XOR gate (sum digit)	
0	*0*	*0*	*0*	*00*
1	*0*	*0*	*1*	*01*
0	*1*	*0*	*1*	*01*
1	*1*	*1*	*0*	*10*

functions as an organizational core. One chromophore is a spiropyran (**1**), and the other two are identical quinoline-derived dihydroindolizines (**2**). The spiropyran in its closed, thermally stable form (**1c**) may be photoisomerized with ultraviolet light (e.g. 355 nm) to an open merocyanine form (**1o**), which thermally closes back to **1c**. Visible light also causes isomerization to **1c**. Each quinoline-derived dihydroindolizine also exists in a thermally stable closed form **2c**. Photoisomerization with ultraviolet light (e.g. 355 nm) produces an open, zwitterionic form that closes thermally, or with visible irradiation. Ignoring stereoisomerism arising from stereocenters in the spiro forms, **122** can in principle exist in six

isomeric forms: **1c2c2c**, **1c2o2c** (where either one of the dihydroindolizines is open), **1c2o2o**, **1o2c2c**, **1o2o2c**, and **1o2o2o**. Only one form, **1c2c2c**, is thermally stable, and any of the other isomers will revert to this form in a few minutes at ambient temperatures. Irradiation of **122** at 355 nm populates all the isomeric forms (Figure 2). Although the details of the kinetic processes are complex, the overall concept is simple: Irradiation at 355 nm leads to net isomerization in the direction of the arrows in Figure 2, whereas thermal reversion results in net isomerization in the opposite direction. In the dark, the entire population is in state **1c2c2c**, at the bottom of the hexagon. Under UV irradiation, the center of the population distribution rises towards the top of the hexagon; at steady-state, the center of this distribution is determined by the equilibria between the thermal and photochemical reactions, which are controlled by the light flux and temperature.

The three chromophores of **122** interact photophysically, and this forms the basis of the half-adder function. The open, merocyanine form of the spiropyran absorbs strongly in the visible (λ_{max} = 579 nm), and is the only chromophore of **122** to fluoresce significantly (λ_{max} = 640 nm). The open form of the quinoline-derived dihydroindolizine absorbs in the same wavelength region as merocyanine emission (λ_{max} = 659 nm), and strongly quenches the merocyanine fluorescence. Thus, of all of the isomeric forms of **122**, only **1c2c2c** is thermally stable, only **1o2c2c** is strongly fluorescent, and only **1o2c2c**, **1o2o2c**, and **1o2o2o** feature the characteristic absorbance of the merocyanine at 579 nm. When **122** is used as a half-adder, inputs *A* and *B* are provided by two light beams at 355 nm with equal intensities. The output of the AND gate (*X*) is the total absorbance at 581 nm (mostly due to **1o2c2c**, **1o2o2c**, and **1o2o2o**), and the output of the XOR gate (*Y*) is the fluorescence of **1o2c2c** at 690 nm, with excitation at 581 nm. Because the AND and XOR gates have the same inputs and operate concurrently, **122** can function as a half-adder.

The half-adder (Figure 3a) consists of a solution of **122** in a suitable solvent, two 355-nm light sources, and apparatus to measure absorbance at 581 nm, and fluorescence at 690 nm with 581-nm excitation. (For convenience, only a single light source was used to provide the two inputs in our

experiments, as described in the Experimental Section.) In AND gate operation, when neither input is *on*, the molecule is in state **1c2c2c**, and no outputs are *on*. When only one input is turned *on*, the total merocyanine concentration rises to a steady-state value determined by the light flux and the thermal reversion rates (Figure 2). This gives rise to some absorption at 581 nm, but the total absorbance is below a threshold level, and does not trigger an *on* response (Figure 3b). When the second input, *B,* is turned *on* instead, the same steady-state absorbance is measured, and the gate remains *off*. However, when both inputs are turned *on* concurrently, the rate of formation of merocyanine increases, but the rate constants for thermal reversion remain unchanged. The center of the isomer distribution rises farther towards the top of the hexagon in Figure 2, and a new, higher steady-state concentration of merocyanine is reached. The absorbance at 581 nm increases above the threshold, and the gate produces an *on* response (Figure 3b). These responses follow the truth table of an AND gate.

The XOR output is merocyanine fluorescence at 690 nm in **1o2c2c**. When 355-nm light is applied to the sample, some **1o2c2c** is formed, leading to an increase in fluorescence at 690 nm. However, if the light flux is increased, **1o2o2c**, and finally **1o2o2o** are generated from **1o2c2c**, and these are essentially nonfluorescent due to quenching by the open dihydroindolizine. The result is that as the 355-nm light intensity is increased from zero, the steady-state fluorescence at 690 nm initially increases, goes through a maximum, and then decreases as the population of quenched isomers increases. In XOR gate operation with two 355-nm inputs, the steady-state emission is therefore significantly *greater* at the *lower* light levels generated by one input than at the higher light levels that are produced when both inputs are turned *on* (Figure 3c). The switching threshold for the XOR gate is exceeded when either input *A* or input *B* is applied, but not when both inputs are applied concurrently; this behavior meets the requirements for an XOR gate. After any combination of inputs, the gate can be reset to **1c2c2c** thermally, or by irradiating with red light.

From the description above, it is evident that a solution of **122** acts as a half-adder: two binary digits, represented by the two inputs, are added (Table 1). The paragraphs below discuss in detail the

preparation of the molecule, the photochemical properties of **122** and two model systems, and the performance and resistance to photochemical degradation of the half-adder.

Synthesis. The core of **122** was prepared from 5-aminoisophthalic acid, whose amino functionality was protected with a *t*-butoxycarbonyl group. The spiropyran acid was prepared as previously described.[19] The precursor of the quinoline-derived dihydroindolizine moieties of **122**, 6-hydroxy-spiro-[9H-fluorene-9,3'(3'aH)-pyrrolo[1,2-a]-quinoline]-1',2'-dicarbonitrile, was prepared using procedures adapted from reported preparations of related compounds.[20] The quinoline-derived dihydroindolizines were coupled to amine-protected 5-aminoisophthalic acid using 3-chloro-4,6-dimethoxy-1,3,5-triazine and N-methylmorpholine. After removal of the protecting group from the resulting dyad, the spiropyran acid was attached using 3-chloro-4,6-dimethoxy-1,3,5-triazine and N-methylmorpholine. Model compounds **3** and **4** (Figure 4) were prepared using similar procedures. Additional information concerning the synthesis and spectroscopic techniques for all compounds is given in the Supporting Information.

Photochemistry of model compounds. In order to understand the photochemical behavior of the triad, we investigated model spiropyran **3** and model dihydroindolizine **4** spectroscopically. The steady-state absorption and emission studies reported below were performed on solutions (~1×10^{-5} M) in 2-methyltetrahydrofuran at 22 ºC, with optical path lengths of 1.0 cm and sample volumes of 1.5 mL.

*Spiropyran **3***. As is the case with other spiropyrans, **3** is thermally stable in the closed, spiro form **3c** (Figure 4). The absorption spectrum of **3c** (Figure 5a) features maxima at 335 and 271 nm. There is no absorption in the visible region of the spectrum. Irradiation at 355 nm causes isomerization to a photostationary distribution containing mainly the merocyanine form **3o** (see Figure 1). The merocyanine has absorption maxima at 593, 334, and 274 nm.

Spiro form **3c** does not fluoresce significantly. Merocyanine **3o** does fluoresce, with λ_{max} = 664 nm (Φ_f = ~0.03) (Figure 5a). Pump-probe transient absorption investigations were performed on **3o**. A 2-methyltetrahydrofuran solution of **3** was constantly irradiated at 366 nm to maintain a photostationary

distribution containing mainly the open form, and the solution was excited at 585 nm with ~100 fs laser pulses. The transient absorption was probed at 720 nm (Figure 6). Three components were observed: a major component (67%) with a lifetime of 45 ±1 ps, a 140 ±10 ps component (19%), and a 0.42 ±0.05 ps component with an amplitude of –14% (grow-in of stimulated emission amplitude with time). Similar results showing the presence of and interconversions between isomers of merocyanines have been observed for other spiropyrans.[18,21-28] Based on studies of a similar molecule,[18] we can assign the 45 ps lifetime in **3o** to the major isomer, which absorbs at 593 nm and emits relatively strongly at 664 nm.

*Quinoline-derived dihydroindolizine **4***. As shown in Figure 5a, the thermally stable, closed form of the dihydroindolizine, **4c**, has absorption maxima in the UV at 393 and 338 nm. After irradiating at 355 nm to generate a photostationary distribution rich in the open, zwitterionic isomer **4o**, new bands appear at 666 and 484 nm. The **4o** isomer does not display any detectable fluorescence. Transient absorption experiments in 2-methyltetrahydrofuran yielded the transient at 720 nm shown in Figure 6. This is ascribed to a mixture of stimulated emission, ground state bleaching, and induced absorption from an unrelaxed ground state. The first excited singlet state of **4o** decays with a time constant of 0.84 ±0.02 ps. A minor component of 2.6 ±0.02 ps is ascribed to induced absorption from an unrelaxed ground state.

Photochemistry of the triad. The absorption spectrum of **1c2c2c** in 2-methyltetrahydrofuran (Figure 5b) shows maxima at 390, 363 (sh), and 272 nm (maximum not shown in Figure). The features at 363 and 272 nm are similar to the absorption bands of model spiropyran **3c**, whereas the 390 nm band is clearly related to the 393 nm band in dihydroindolizine model **4c** (Figure 5a). Thus, the triad absorption is consistent with a superposition of the bands of the component chromophores. Irradiation of the sample of **1c2c2c** at 355 nm results in the appearance of new bands at 659, 579 and 485 nm (Figure 5b). The 659 and 485 nm bands are similar to those of the open form of the dihydroindolizine model **4o** whereas the 579 nm band is similar to the 593-nm band of **3o**. Thus, irradiation of **1c2c2c** with ultraviolet light generates a photostationary distribution containing significant amounts of the open forms of the chromophores. The amplitude in the 700 – 750 nm region is a function of the amount of open dihydroindolizine present, whereas the amplitude in the 580-nm region reflects mainly the amount

of the merocyanine form of the spiropyran. The only fluorescence emission observed from **122** is from the merocyanine form of the spiropyran, with a maximum at 640 nm.

Isomerization kinetics. The thermal closing kinetics of the photochromes in **122** were investigated. A sample of **1c2c2c** in 2-methyltetrahydrofuran at 22 ºC was irradiated at 355-nm to prepare a solution enriched in the open isomers, the light was extinguished, and the absorbance as a function of time was monitored. Time constants for the exponential thermal isomerizations were 160 s for the spiropyran and 189 s for the dihydroindolizine. Both isomerization rates significantly increased with visible light irradiation ($580 \leq \lambda \leq 900$ nm, ~50 mW/cm^2) because photochemical closing contributed. Photochemical opening rates were studied using 355 nm light from a Nd:YAG pulsed laser operated at 10 Hz. The average total power of the beam striking the sample was 28 mW. Time constants for opening of the spiropyran and dihydroindolizine were 4.4 and 5.1 s, respectively. When the average light flux was reduced by a factor of two by slowing the laser repetition rate to 5 Hz (14 mW average total power), the corresponding time constants were 7.9 s and 8.5 s. At the lower light flux, the photoisomerization rates are not decreased by a factor of two because thermal closing competes with the photochemical opening, and the thermal rate constants do not change with light flux.

Absorbance as a function of isomerization rates. Figure 7a shows the time dependence of the absorbance of **122** in 2-methyltetrahydrofuran under exposure to 355-nm light. At zero time, the sample consisted completely of **1c2c2c.** The solid line shows the absorbance at 581 nm, where most of the absorbance is due to the merocyanine form of the spiropyran, when the sample was exposed to 355-nm laser pulses at 5 Hz (14 mW average power). The absorbance rises from virtually zero when the light is turned on at 0 s, reaching a steady-state value after about 35 s. The absorbance at any time reflects the sum of the concentrations of the three isomers of **122** that contain the merocyanine. When the light is first turned on, the population distribution (Figure 2) favors **1o2c2c** and **1c2o2c**. As irradiation is continued, the population shifts towards the top of the hexagon in Figure 2, and **1o2o2c** and **1o2o2o** make greater contributions to the absorbance at 581 nm. After 35 s, a steady-state distribution is

attained. The fraction of each of the six isomers is determined not only by the various rate constants for photoinduced opening and closing, but also the rate constants for thermal closing.

The dotted line in Figure 7a shows the results of a similar experiment carried out with the laser at a repetition rate of 10 Hz (28 mW average power). The concentration of merocyanine initially rises at about twice the rate observed in the first experiment, as expected. The steady-state concentration is higher because the rates of photochemical opening of the spiropyran (and photochemical closing) increase due to the doubled laser power, but the thermal closing rate constants are not changed, moving the steady-state distribution of isomers farther toward the top of the hexagon. As will be discussed later, this phenomenon forms the basis of the AND gate function.

Fluorescence as a function of isomerization rates. Figure 7b shows the results of a similar experiment in which the emission intensity of the merocyanine at 690 nm (excitation at 581 nm) was monitored. Prior to excitation, there is no appreciable fluorescence because essentially no merocyanine is present. With 355-nm excitation at 5 Hz (solid line), the emission intensity increases rapidly as some of the sample is converted to **1o2c2c**, which is the only isomer that is significantly fluorescent. After about 3 s the emission intensity begins to decrease because **1o2c2c** is being converted into **1o2o2c**, some of which in turn is converted to **1o2o2o**. Both of these latter isomers are virtually non-fluorescent due to quenching of the merocyanine excited states by the open dihydroindolizine moieties. After about 30 s, a constant emission level is reached, which is established by the steady-state distribution of the population among the six isomers. Thus, upon exposure to 355-nm light, emission from **122** increases to a maximum and then decreases to a steady-state value. This kind of "off–on-off" behavior has been termed "neuronal," because it resembles that of the chemical synapses of neurons. Several examples of neuronal behavior in molecular systems have been reported.[29-34]

When the average light flux is doubled by doubling the repetition rate of the laser to 10 Hz, the fluorescence intensity as a function of time is different (dotted line, Figure 7b). Due to the higher light flux, the emission at 690 nm increases more rapidly than in the 5-Hz experiment because **1o2c2c** is formed more rapidly from **1c2c2c**. However, the intensity maximum is reached sooner, as the rates of

formation of **1o2o2c** and **1o2o2o** are also increased. Most importantly, the steady-state emission intensity is *lower* than that observed with lower light flux. The reason is that with the higher flux, the steady-state distribution of isomers contains a higher fraction of the quenched isomers **1o2o2c** and **1o2o2o**, which are formed at the expense of the emissive **1o2c2c**. This inverse behavior, where increased light intensity leads to lower emission intensity, forms the basis of the XOR gate.

The quenching process. It is clear from the data that the open forms of the dihydroindolizine of **122** quench the fluorescence of the merocyanine form of the spiropyran. Information concerning the kinetics of this quenching was obtained from time-resolved transient absorbance studies with excitation at 585 nm by ca. 100 fs laser pulses, during which time the sample was continuously irradiated at 366 nm in order to assure a population of isomers containing the merocyanine and the open forms of the dihydroindolizines. The population of the merocyanine first excited singlet state was monitored via its stimulated emission at 720 nm (Figure 6).[18] Because the steady-state population contains six different forms of the triad, and because, as discussed above, the model spiropyran and dihydroindolizine molecules themselves display multiple excited state decay processes, it is not practical to interpret these data in terms of specific concentrations and rate constants. However, it is obvious from Figure 6 that linking the chromophores to form the triad does introduce new decay components that are not present in the model compounds. In particular, a new component with a lifetime on the 3 ps time scale is observed. The data for the first 10 ps of the transient decay could be fitted with three exponential processes: 45 ps (40% of the decay, fixed lifetime based on results for model merocyanine **3o**), 0.84 ps (30%, fixed lifetime based on model open dihydroindolizine **4o**) and 3 ±1 ps (30%). The 3-ps component is ascribed to quenching of the merocyanine excited singlet state. Because the relative populations of **1o2o2c** and **1o2o2o** under the conditions of the experiment are not known, we do not know whether this value is characteristic of one of these isomers, or an unresolved mixture of time constants for both. In addition, the above analysis is oversimplified, as the decay kinetics, especially at longer times (not shown), contain additional components, as discussed above. The important point is that the results are consistent with the strong quenching of the merocyanine excited singlet state that was discussed above, because

the relevant lifetimes of the merocyanine excited states observed in model compound **3o** were 45 and 140 ps.

The nature of the quenching process is not immediately apparent. Singlet-singlet energy transfer or photoinduced electron transfer are the most likely mechanisms, and the spectroscopic data do not allow us to strictly rule out either process. However, photoinduced electron transfer seems unlikely. The first oxidation potential of merocyanine **3o** is 1.20 V vs SCE, and the first reduction potential is –1.25 V.[18] Cyclic voltammetric measurements of model dihydroindolizine **5o** yielded a first oxidation potential of 0.75 V, and a first reduction potential of –0.70 V. Thus, the lowest-energy charge-separated state in **122** would contain a merocyanine radical cation and an open dihydroindolizine radical anion, and would have an energy of ca. 1.9 eV above that of the ground state. The energy of the excited state of the merocyanine is ca. 2.0 eV. Photoinduced electron transfer would have a thermodynamic driving force of ca. 100 mV. It seems unlikely that this process would occur on the 3 ps time scale. On the other hand, the excellent overlap between the emission of the merocyanine and the absorption of the open dihydroindolizine (Figure 5), coupled with the short distance between the chromophores, suggests that singlet-singlet energy transfer by the Förster mechanism would be extremely efficient. We therefore expect that energy transfer is the most likely quenching process. In any case, the nature of the quenching is not actually relevant for the performance of the device, which simply requires that quenching of some sort occur.

Performance as a half-adder. Given the discussion of triad photochemistry presented above, it is clear that **122** can act as a single-molecule half-adder with all-photonic inputs and outputs. As illustrated in Figure 3a, the two inputs, shared by both the AND and XOR gate functions, are light at 355 nm. In principle, these could be two steady-state light sources of equal intensity, but in this work we used a pulsed laser operating at 5Hz (for input *A* or input *B*; 14 mW average power) or 10 Hz (for both inputs on concurrently, 28 mW average power) for the sake of convenience. The output for the AND gate is the absorbance of the merocyanine in **1o2c2c**, **1o2o2c**, and **1o2o2o** monitored at 581 nm. The output for the XOR gate is emission of the merocyanine in **1o2c2c**, excited at 581 nm and monitored at 690 nm.

Although in principle both outputs could be induced by the same 581-nm analyzing light and measured with photodiodes having suitable geometries and interference filters, we measured them separately using a fluorimeter and absorbance spectrophotometer. In our implementation of the half-adder, both outputs were obtained 6.5 s after the input(s) were turned on, as this arrangement was convenient and gave good signal-to-noise ratios. From Figure 7 it is clear that the outputs could have been read at any later time, as long as the inputs were left on until the outputs were determined.

In operation, the initial state of the half-adder is **1c2c2c**. This is the only significant species present in the dark at thermal equilibrium, and the system may be reset to this state after application of any combination of inputs by irradiation with red light ($580 \leq \lambda \leq 900$ nm). In this state, no visible-absorbing isomers are present, and both outputs are *off*, representing the addition of *0* and *0* to give *00* in binary (Figures 3b and c). If either input is turned *on*, the absorbance at 581 nm rises to a steady-state value, signaling formation of merocyanine. However, the threshold for an *on* response of the AND gate is set at a higher amplitude than this, so the AND gate remains *off*. With one input *on*, the emission of the merocyanine rises to a value above the threshold, signaling an *on* response of the XOR gate. Thus, the half-adder adds *0* and *1* (or *1* and *0*) to give *01*. Finally, if both inputs are turned *on*, the absorbance at 581 increases to a value above the threshold because additional merocyanine-containing species are produced. The AND gate yields an *on* output. The fluorescence at 690, however, is *lower* than that observed for only one input, due to fluorescence quenching, and the XOR output is *off*. Thus, the half-adder output is *10*, or 2 in base-10 arithmetic. Figures 3b and c show the actual response levels attained in these experiments. The absorbance and emission data are essentially noise free under these conditions (Figure 7).

Cycling and photodecomposition. To be useful in any real-world application, a molecular arithmetic device must be capable of cycling through its various states numerous times. Although the intent of this work is to demonstrate function, and not to produce a technological device, we did investigate the stability of **122** when cycling. Figure 8a shows the absorbance at 581 nm during a sequence of 10 reset ($580 \leq \lambda \leq 900$ nm, ca. 50 mW/cm^2, 10 min), single input (355 nm laser pulses at 5 Hz, 14 mW average

power, 6.5 s), and dual input (355 nm laser pulses at 10 Hz, 28 mW average power, 6.5 s) exposures and readout operations. There is little or no degradation within the variations of the measurements. Figure 8b shows the emission at 690 nm following the same series of inputs and resetting operations. Again, little or no degradation is observed. Thus, the material is stable under these conditions when rigorously deoxygenated.

Conclusions

Triad **122** functions as a one-molecule Boolean half-adder with all-photonic inputs and outputs. It is stable and capable of cycling many times. The instrumentation required for operation is very simple, consisting, in principle, of two identical steady-state light sources as inputs, a single light source for readout, and two diode detectors to measure absorbance and emission changes at suitable wavelengths. Incorporation of both the AND and XOR functions into the same molecule greatly simplifies the system. The chemical linkage between the chromophores permits rapid and efficient quenching of the merocyanine excited state by the open dihydroindolizine, making the XOR function possible.

The cycle times are dependent upon the inputs. The time constants for the various photochemical reactions are on the ns time scale or less, and the time required to reach steady state depends upon the intensity of the exciting light. In the experiments reported here, total irradiation times (with 5 ns pulses) were on the order of a few hundred ns. If readout is performed only after steady-state conditions are reached (Figure 7), it is clear that thermal isomerization times will limit the device speed, and these will be governed by the temperature. However, from Figure 7 it is apparent that there is no need to wait until equilibrium is achieved in order to obtain adequate signal-to-noise ratios. Under the conditions employed, clear response differences are apparent in as few as 6 s after inputs are turned *on*. One disadvantage of this system is that the inputs must be *on* during readout, or turned *off* immediately prior to readout. Because of thermal reversion to the *off* form, the molecule does not record its state for more than a few minutes at room temperature after application of inputs ceases.

The system has several advantages over molecular arithmetic systems that depend upon addition of chemicals for some or all of the inputs. No physical access for materials to the volume element containing the half-adder is required, fluid solutions are not required, diffusional processes do not play a role, and resetting is possible without the buildup of side products and dilution that could eventually interfere with the operation of the system. Although this triad successfully demonstrates the function of a molecular half-adder, the usefulness of such molecular logic in real-world applications has yet to be determined.

Acknowledgment. This work was supported by the Swedish Research Council (VR) and the U. S. National Science Foundation (CHE-0352599). This is publication 669 from the ASU Center for the Study of Early Events in Photosynthesis.

Supporting Information Available: Synthesis and characterization of the compounds described herein and the conditions for performance of the optical studies are available free of charge via the Internet at http://pubs.acs.org.

References

(1) Andréasson, J.; Kodis, G.; Terazono, Y.; Liddell, P. A.; Bandyopadhyay, S.; Mitchell, R. H.; Moore, T. A.; Moore, A. L.; Gust, D. *J. Am. Chem. Soc.* **2004**, *126*, 15926-15927.

(2) de Silva, A. P.; McClenaghan, N. D. *J. Am. Chem. Soc.* **2000**, *122*, 3965-3966.

(3) Guo, X.; Zhang, D.; Zhang, G.; Zhu, D. *J. Phys. Chem. B* **2004**, *108*, 11942-11945.

(4) Margulies, D.; Melman, G.; Felder, C. E.; Arad-Yellin, R.; Shanzer, A. *J. Am. Chem. Soc.* **2004**, *126*, 15400-15401.

(5) Margulies, D.; Melman, G.; Shanzer, A. *Nature Materials* **2005**, *4*, 768-771.

(6) Qu, D. H.; Wang, Q. C.; Tian, H. *Angew.e Chem. Int. Ed.* **2005**, *44*, 5296-5299.

(7) Stojanovic, M. N.; Stefanovic, D. *J. Am. Chem. Soc.* **2003**, *125*, 6673-6676.

(8) Coskun, A.; Deniz, E.; Akkaya, E. U. *Org. Lett.* **2005**, *7*, 5187-5189.

(9) Langford, S. J.; Yann, T. *J. Am. Chem. Soc.* **2003**, *125*, 11198-11199.

(10) Remacle, F.; Speiser, S.; Levine, R. D. *J. Phys. Chem. B* **2001**, *105*, 5589-5591.

(11) Remacle, F.; Weinkauf, R.; Levine, R. D. *J. Phys. Chem. A* **2006**, *110*, 177-184.

(12) Gust, D.; Moore, T. A.; Moore, A. L. *Chem. Commun.* **2006**, *2006*, 1169-1178.

(13) Andréasson, J.; Terazono, Y.; Albinsson, B.; Moore, T. A.; Moore, A. L.; Gust, D. *Angew. Chem. Int. Ed.* **2005**, *44*, 7591-7594.

(14) Terazono, Y.; Kodis, G.; Andréasson, J.; Jeong, G.; Brune, A.; Hartmann, T.; Dürr, H.; Moore, A. L.; Moore, T. A.; Gust, D. *J. Phys. Chem. B* **2004**, *108*, 1812-1814.

(15) Liddell, P. A.; Kodis, G.; Andréasson, J.; de la Garza, L.; Bandyopadhyay, S.; Mitchell, R. H.; Moore, T. A.; Moore, A. L.; Gust, D. *J. Am. Chem. Soc.* **2004**, *126*, 4803-4811.

(16) Straight, S. D.; Andréasson, J.; Kodis, G.; Bandyopadhyay, S.; Mitchell, R. H.; Moore, T. A.; Moore, A. L.; Gust, D. *J. Am. Chem. Soc.* **2005**, *127*, 9403-9409.

(17) Straight, S. D.; Andréasson, J.; Kodis, G.; Moore, A. L.; Moore, T. A.; Gust, D. *J. Am. Chem. Soc.* **2005**, *127*, 2717-2724.

(18) Bahr, J. L.; Kodis, G.; de la Garza, L.; Lin, S.; Moore, A. L.; Moore, T. A.; Gust, D. *J. Am. Chem. Soc.* **2001**, *123*, 7124-7133.

(19) Garcia, A. A.; Cherian, S.; Park, J.; Gust, D.; Jahnke, F.; Rosario, R. *J. Phys. Chem. A* **2000**, *104*, 6103-6107.

(20) Dürr, H. Photochromism of dihydroindolizines and related systems; In *Organic Photochromic and Thermochromic Compounds*; Crano, J. C., Guglielmetti, R. J., eds. Plenum Press: New York, 1999; pp 223-266.

(21) Wohl, C. J.; Kuciauskas, D. *J. Phys. Chem. B* **2005**, *109*, 22186-22191.

(22) Heiligman-Rim, R.; Hirshberg, Y.; Fischer, E. *J. Phys. Chem.* **1962**, *66*, 2465-2477.

(23) Takahashi, H.; Yoda, K.; Isaka, H.; Ohzeki, T.; Sakaino, Y. *Chem. Phys. Lett.* **1987**, *140*, 90-94.

(24) Hobley, J.; Malatesta, V. *Phys. Chem. Chem. Phys.* **2000**, *2*, 57-59.

(25) Abel, Y.; Nakao, R.; Horii, T.; Okada, S.; Irie, M. *J. Photochem. Photobiol. A* **1996**, *95*, 209-214.

(26) Cottone, G.; Noto, R.; La Manna, G.; Fornili, S. L. *Chem. Phys. Lett.* **2000**, *2000*, 51-59.

(27) Wilkinson, F.; Worrall, D. R.; Hobley, J.; Jansen, L.; Williams, S. L.; Langley, A. J.; Matousek, P. *J. Chem. Soc. , Faraday Trans.* **1996**, *92*, 1331-1336.

(28) Marevtsev, V. S.; Zaichenko, N. L. *J. Photochem. Photobiol. A* **1997**, *104*, 197-202.

(29) Callan, J. F.; de Silva, A. P.; McClenaghan, N. D. *Chem. Commun.* **2004**, 2048-2049.

(30) deSilva, A. P.; Gunaratne, H. Q. N.; McCoy, C. P. *Chem. Commun.* **1996**, 2399-2400.

(31) Fabbrizzi, L.; Gatti, F.; Pallavicini, P.; Parodi, L. *New J. Chem.* **1998**, *22*, 1403-1407.

(32) Gunnlaugsson, T.; Leonard, J. P.; Senechal, K.; Harte, A. J. *J. Am. Chem. Soc.* **2003**, *125*, 12062-12063.

(33) Pallavicini, P.; Amendola, V.; Massera, C.; Mundum, E.; Taglietti, A. *Chem. Commun.* **2002**, 2452-2453.

(34) Pina, F.; Melo, M. J.; Maestri, M.; Passaniti, P.; Balzani, V. *J. Am. Chem. Soc.* **2000**, *122*, 4496-4498.

Figure Captions

Figure 1. Structure of triad **122** and isomerization of the spiropyran (**1**) and quinoline-derived dihydroindolizine (**2**) photochromes.

Figure 2. Graph of isomerization pathways for **122**. Net photochemical isomerization under the influence of UV light occurs in the direction of the arrows. Thermal isomerization and photoisomerization promoted by visible light occurs in the opposite direction.

Figure 3 (a) Schematic diagram of the half-adder. (b) Actual performance of the AND gate function under the application of various combinations of inputs. (c) Performance of the XOR gate function. For signal-to-noise ratios in the absorption and emission readout processes, and for reproducibility of the data from one experiment to another, see Figures 7 and 8, respectively.

Figure 4. Structures of the closed, spiro forms of model spiropyran **3c** and model quinoline-derived dihydroindolizines **4c** and **5c.** The structures of the open forms (**3o**, **4o**, **5o**) are analogous to those of the corresponding structures in **1o** and **2o** (Figure 1).

Figure 5. (a) Absorption spectra of **3c** (red dots), a photostationary distribution containing mainly **3o** (red line), **4c** (green dots), a photostationary distribution containing mainly **4o** (green line), and emission spectrum of **3o** (red dashes). (b) Absorption spectra of **1c2c2c** (blue line), and the same solution after irradiation at 355 nm to generate a photostationary distribution rich in the open forms of the triad (red line).

Figure 6. Transient absorption kinetics at 720 nm following excitation with a 585 nm, ca. 100 fs, laser pulse during constant illumination of the sample at 366 nm. Data for model compounds **3** (□) and **4** (○) and triad **122** (◊) are shown. The figure shows the negative of the absorbance change on a natural logarithm scale for the first 7 ps of the observation period. The solid line is a multi-exponential fit to the

data for **122**, as discussed in the text. The ΔA values have been normalized for ease in comparison of the kinetics; the actual values are ≤ -0.03.

Figure 7. (a) Absorbance of a solution of **122** in 2-methyltetrahydrofuran at 581 nm as a function of irradiation time with 355 nm laser pulses having a repetition rate of 5 Hz (——) or 10 Hz (• • • •). (b) Fluorescence of a solution of **122** in 2-methyltetrahydrofuran at 690 nm (λ_{ex} = 581 nm) as a function of irradiation time with 355 nm laser pulses having a repetition rate of 5 Hz (——) or 10 Hz (• • • •).

Figure 8. Cycling of the triad. (a) Absorbance at 581 nm following reset (580 ≤ λ ≤ 900 nm, ca. 50 mW/cm^2, 10 min) (black), irradiation with one input (355 nm laser pulses at 5 Hz, 14 mW average power, 6.5 s) (red) and irradiation with both inputs (355 nm laser pulses at 10 Hz, 28 mW average power, 6.5 s) (green). (b) Emission at 690 nm (581 nm excitation) following the same sequence of irradiations.

Figure 1

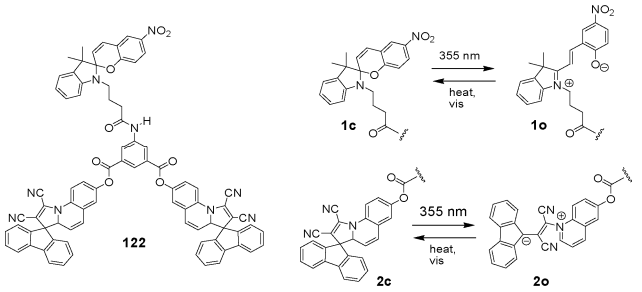

Figure 2

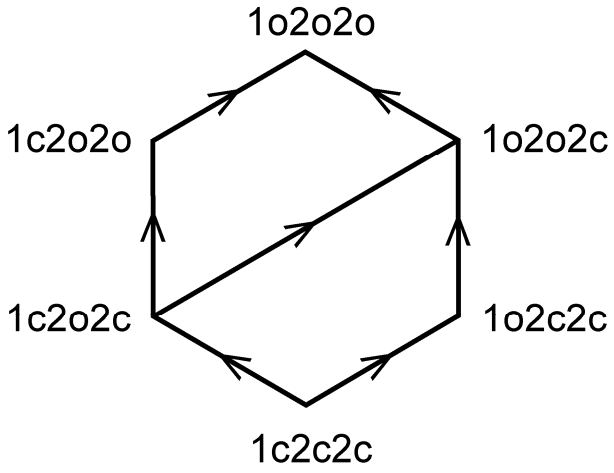

Figure 3

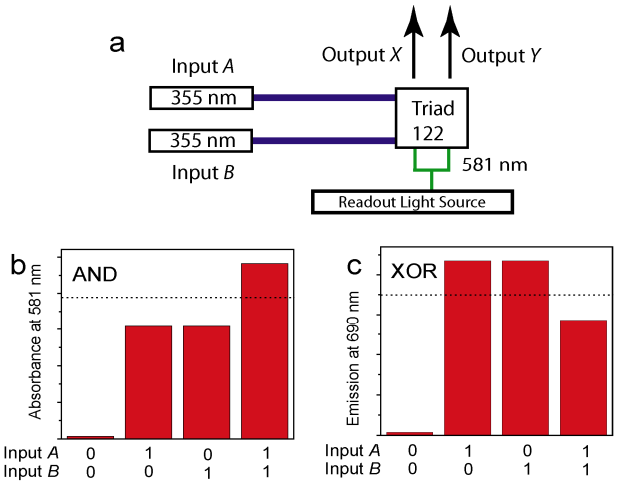
a
Input A
355 nm
355 nm
Input B
Output X
Output Y
Triad
122
581 nm
Readout Light Source
b
AND
Absorbance at 581 nm
Input A 0 1 0 1
Input B 0 0 1 1
c
XOR
Emission at 690 nm
Input A 0 1 0 1
Input B 0 0 1 1

Figure 4

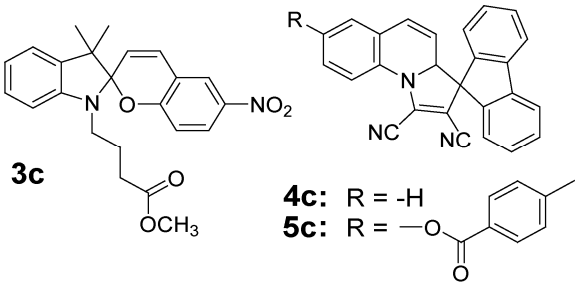

Figure 5

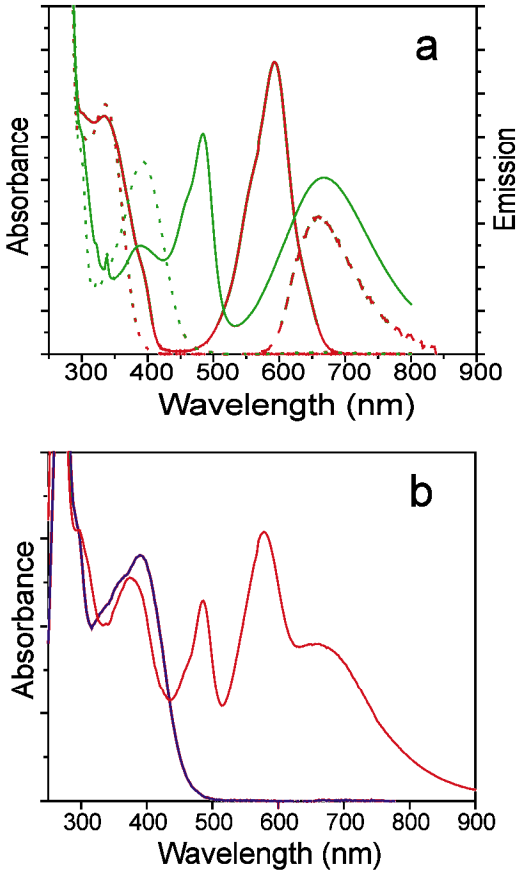
a
Absorbance
Emission
300
400
500
600
700
800
900
Wavelength (nm)
b
Absorbance
300
400
500
600
700
800
900
Wavelength (nm)

Figure 6

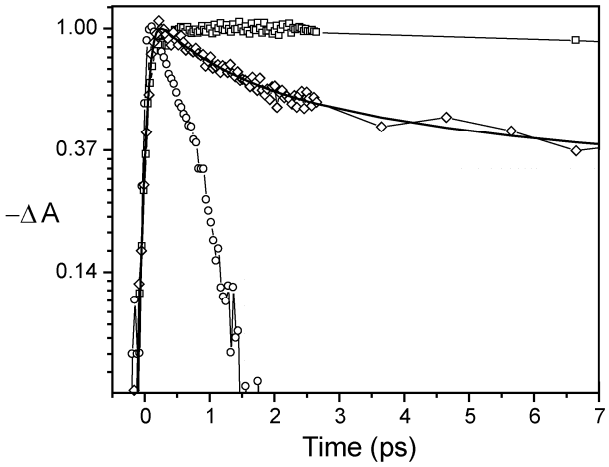

Figure 7

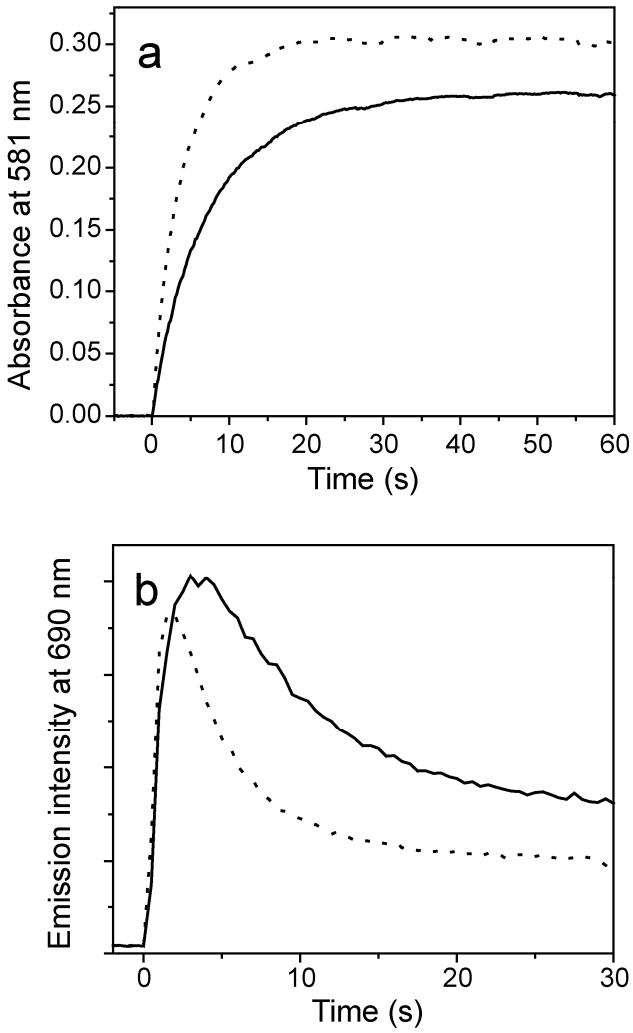
a
Absorbance at 581 nm
0.00
0.05
0.10
0.15
0.20
0.25
0.30
0
10
20
30
40
50
60
Time (s)
b
Emission intensity at 690 nm
0
10
20
30
Time (s)

Figure 8

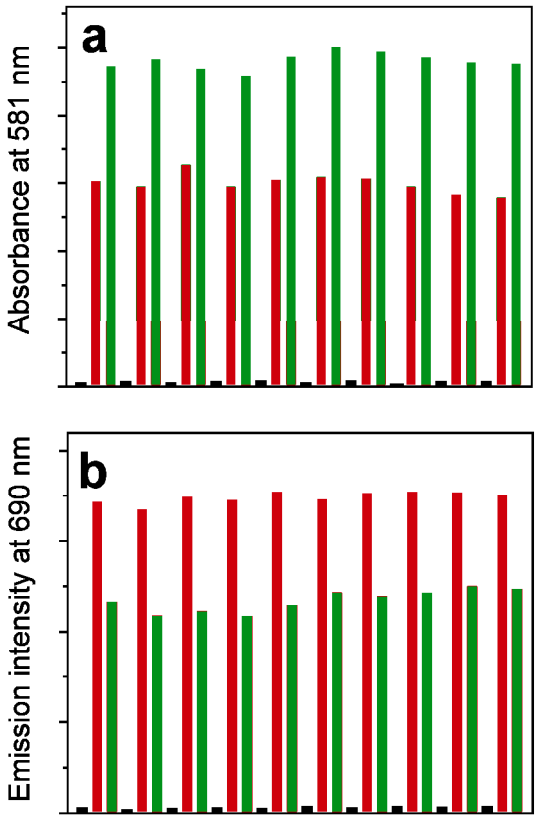

TOC Graphic